

Annex 1

A1.1: General Processing Roadmap

The radiometric interoperability of CEOS ARD SAR products is ensured by a common processing chain during production. The recommended processing roadmap involves the following steps:

- Apply the best possible orbit parameters to give the most accurate product possible. These will have been projected to an ellipsoidal model such as WGS84. In order to achieve the level of geometric accuracy required for the DEM-based correction, precise orbit determination will be required.
- Apply instrument calibration to produce Beta-Nought values with high fidelity.
- Convert Single-Look-Complex (SLC) radiometric channel(s) to intensity **[NRB]**, **[ORB]** and **[POL]** and in addition for **[POL]**, the cross-product element(s) of the covariance as shown in Annex 2.1.
- Perform radiometric terrain correction (gamma backscatter convention terrain-flattening) on the covariance matrix by applying the local surface normalisation factor to each backscatter measurement element (Small, 2011, Shiroma et al., 2022).
- Perform polarimetric speckle filtering (optional for **[NRB]** and **[ORB]**), before geocoding, in order to optimally preserve the polarimetric information. Most popular polarimetric decomposition methodologies are incoherent in nature, which requires averaging the covariance matrix for stationarity. Depending on the application, a polarimetric filter that preserves local point targets and locally average extended targets may be used, e.g., Sigma Lee filter with 7x7 window and 3-point target (Lee et al., 2009). Multi-looking could be performed to meet optimal output sample spacing before the geometric correction step. No speckle filtering or multi-looking is performed for **[GSLC]** products.
- For **[GSLC]** products, the topographic phase is estimated relative to a reference orbit and removed from the SLC data (Zebker et al. 2010, Zebker, 2017) (see Annex A1.2)
- Geometric terrain correction (relative to geoid for **[ORB]**) is applied to the normalized backscatter measurement data. For **[POL]**, the resampling methodology should be nearest-neighbour, bilinear or average in order to preserve integrity of the covariance matrix as other resampling functions can introduce artefacts due to the mix of intensity and complex number elements in the matrix. Geocoding to a common grid structure with specified pixel spacings for true data cube format.
- Generate CEOS format metadata to accompany product layers.
- Optionally, a Spatio Temporal Asset Catalog (STAC) file is added to the product.

Table A1 lists possible sequential steps and , existing software tools (e.g. Gamma software (GAMMA, 2018)) and scripting tasks that can be used to form the CEOS ARD SAR processing roadmap.

Table A1 SAR ARD PR processing roadmap and software options. RADARSAT-2 Example

Step	Implementation option
1. Orbital data refinement	Check xml date and delivered format. RADARSAT-2, pre EDOT (July 2015) replace. Post July 2015, check if 'DEF', otherwise replace. (Gamma - RSAT2_vec)
2. Apply radiometric scaling Look-Up Table (LUT) to Beta-Nought	Specification of LUT on ingest. (Gamma - par_RSAT2_SLC/SG)
3. Generate covariance matrix elements	Gamma – COV_MATRIX
4. Radiometric terrain normalisation	Gamma - geo_radcal2
5. Speckle filtering (Boxcar or Sigma Lee)	Custom scripting
6. Geometric terrain correction/Geocoding	Gamma – gc_map and geocode_back
7. Create metadata	Custom scripting

A1.2: Topographic phase removal

InSAR analysis capabilities from CEOS ARD SAR products are enabled with [GSLC] products, which is also the case when the Flattened Phase per-pixel data (item 3.7) are included in the [NRB] or [POL] products. This is made possible since the simulated topographic phase relative to a given reference orbit has been subtracted.

From classical approach with SLC data, interferometric phase $\Delta\varphi_{1-2}$ between two SAR acquisitions is composed of a topographic phase $\Delta\varphi_{Topo_{1-2}}$, a surface displacement phase $\Delta\varphi_{Disp_{1-2}}$ and other noise terms $\Delta\varphi_{Noise_{1-2}}$ [Eq.1]. The topographic phase consists to the difference in geometrical path length from each of the two antenna positions to the point on the SAR image (φ_{DEM_SLC}) and is a function of their orbital baseline distance [Eq.2]. The surface displacement phase is related to the displacement of the surface that occurred in between the two acquisitions. The noise term is the function of the radar signal interaction with the atmosphere and the ionosphere during each acquisition and function of the system noise.

$$\Delta\varphi_{1-2} = \Delta\varphi_{Topo_{1-2}} + \Delta\varphi_{Disp_{1-2}} + \Delta\varphi_{Noise_{1-2}} \quad \text{Eq. 1}$$

Where

$$\Delta\varphi_{Topo_{1-2}} = \varphi_{DEM_SLC_1} - \varphi_{DEM_SLC_2} \quad \text{Eq. 2}$$

Since CEOS ARD products are already geocoded, it is important to remove the wrapped simulated topographic phase φ_{SimDEM_SLC} from the data in slant range during their production, before the geocoding step [Eq.3]. The key here is to simulate the topographic phase relatively to a constant reference orbit, as done in a regular InSAR processing. There are two different ways to simulate the topographic phase:

- 1- The use of a virtual circular orbit above a nonrotating planet [Zebker et al. 2010]
- 2- The use of a specific orbit cycle or a simulated orbit of the SAR mission.

In both cases, the InSAR topographic phase $\Delta\varphi_{Topo_OrbRef-2}$ is simulated against the position of a virtual sensor φ_{DEM_OrbRef} lying on a reference orbit, instead of being simulated relatively to an existing reference SAR acquisition ($\varphi_{DEM_SLC_1}$). The use of a virtual circular orbit is a more robust approach since the reference orbit is defined at a fixed height above scene nadir and assuming the reference orbital height constant for all CEOS ARD products. While with the second approach, the CEOS ARD data producer must select a specific archived orbit cycle of the SAR mission or define a simulated one, from which the relative orbit, matching the one of the SAR acquisitions to be processed (to be converted to CEOS ARD), is defined as the reference orbit. With this second approach, it is important to always use the same orbit cycle (or simulated orbit) for all the CEOS ARD produced for a mission, in order to preserve the relevant compensated phase in between them. Providing absolute reference orbit number information in the metadata (item 1.7.15) allows users to validate the InSAR feasibility in between CEOS ARD products.

$$\varphi_{Flattened_SLC_2} = \varphi_{SLC_2} - \Delta\varphi_{Topo_OrbRef-2} \quad \text{Eq. 3}$$

This procedure is equivalent to bring the position of the sensor platform of all the SAR acquisitions at the same orbital position (i.e., zeros baseline distance in between), which results in a Flattened phase $\varphi_{Flattened_SLC}$, independent of the local topography.

The phase subtraction could be performed by using a motion compensation approach (Zebker et al 2010) or directly on the SLC data. Then the geometrical correction is performed on the Flattened SLC which results in a **[GSLC]** product.

[GSLC] can also be saved as a **[NRB]** product by including the Flattened Phase per-pixel data (item 3.7) as follows:

$$NRB: \gamma_T^o = |GSLC|^2$$

$$Flattened \text{ Phase: } \varphi_{Flattened} = arg(GSLC)$$

For **[POL]** product, the Flattened phase needs also to be subtracted from the complex number phase of the off-diagonal elements of the covariance matrix.

Demonstration:

From CEOS ARD flattened SAR products, InSAR processing can be easily performed without dealing with topographic features and orbital sensor position, as for example with two **[GSLC]** products

$$\begin{aligned} \varphi_{Flattened_GSLC_1} &= \varphi_{SLC_1} - \Delta\varphi_{Topo_OrbRef-1} = \varphi_{SLC_1} - \varphi_{DEM_OrbRef} - \varphi_{DEM_SLC_1} \\ \varphi_{Flattened_GSLC_2} &= \varphi_{SLC_2} - \Delta\varphi_{Topo_OrbRef-2} = \varphi_{SLC_2} - \varphi_{DEM_OrbRef} - \varphi_{DEM_SLC_2} \end{aligned} \quad \text{Eq. 4}$$

The differential phase is

$$\Delta\varphi_{CARD_1-CARD_2} = \varphi_{Flattened_GSLC_1} - \varphi_{Flattened_GSLC_2} \quad \text{Eq. 5}$$

Which can be expanded using [Eq.3]

$$\Delta\varphi_{CARD_1-CARD_2} = (\varphi_{SLC_1} - \varphi_{DEM_OrbRef} - \varphi_{DEM_SLC_1}) - (\varphi_{SLC_2} - \varphi_{DEM_OrbRef} - \varphi_{DEM_SLC_2}) \quad \text{Eq. 6}$$

$$\Delta\varphi_{CARD_1-CARD_2} = (\varphi_{SLC_1} - \varphi_{SLC_2}) - (\varphi_{DEM_SLC_1} - \varphi_{DEM_SLC_2}) \quad \text{Eq. 7}$$

$$\Delta\varphi_{CARD_1-CARD_2} = \Delta\varphi_{SLC_1-SLC_2} - \Delta\varphi_{Topo_1-2} \quad \text{Eq. 8}$$

Where $\Delta\varphi_{SLC_1-SLC_2}$ can be express as equation 1, which gives

$$\Delta\varphi_{CARD_1-CARD_2} = (\Delta\varphi_{Topo_1-2} + \Delta\varphi_{Disp_1-2} + \Delta\varphi_{Noise_1-2}) - \Delta\varphi_{Topo_1-2} \quad \text{Eq. 9}$$

Consequently, the differential phase of two CEOS_ARD products doesn't contain a topographic phase, and is already unwrapped (at least over stable areas). It is only function of the surface displacement and of the noise term. Depending on the reference DEM and the satellite orbital state vector accuracies, some residual topographic phase could be present. Atmospheric (item 2.15) and ionospheric (item 2.16) phase corrections could be performed during the production of CEOS ARD products, which reduces the differential phase noise in an InSAR analysis.

$$\Delta\varphi_{CARD_1-CARD_2} = \Delta\varphi_{Disp_1-2} + \Delta\varphi_{Noise_1-2} \quad \text{Eq. 10}$$

Annex 2: Polarimetric Radar [POL]

A2.1 Normalised Covariance Matrices (CovMat)

In order to preserve the inter-channel polarimetric phase and thus the full information content of coherent dual-pol and fully polarimetric data, the covariance matrix is proposed as the data storage format. Covariance matrices are generated from the complex cross product of polarimetric channels, as shown in Equation 1 for fully polarimetric data (C3) and in Equation 2 for dual polarization data (C2). Since these matrices are complex symmetrical, only the upper diagonal elements (bold elements) need to be stored in the ARD database.

Fully polarimetric

$$C3 = \begin{bmatrix} |HH|^2 & \sqrt{2} \cdot HH \cdot HV^* & HH \cdot VV^* \\ \sqrt{2} \cdot HV \cdot HH^* & 2 \cdot |HV|^2 & \sqrt{2} \cdot HV \cdot VV^* \\ VV \cdot HH^* & \sqrt{2} \cdot VV \cdot HV^* & |VV|^2 \end{bmatrix} \quad \text{Eq. 1}$$

Where $HV = VH$, under the reciprocity assumption. $| |$ and $*$ mean respectively complex modulus and the complex conjugate.

Dual polarization

HH-HV

$$C2 = \begin{bmatrix} |HH|^2 & HH \cdot HV^* \\ HV \cdot HH^* & |HV|^2 \end{bmatrix} \quad \text{or}$$

VV-VH

$$C2 = \begin{bmatrix} |VH|^2 & VH \cdot VH^* \\ VH \cdot VH^* & |VV|^2 \end{bmatrix} \quad \text{or}$$

Eq. 2

CH-CV

$$C2 = \begin{bmatrix} |CH|^2 & CH \cdot CV^* \\ CV \cdot CH^* & |CV|^2 \end{bmatrix}$$

Where CH and CV refer to dual polarization transmitting a circular polarized signal. [CH, CV] can be replaced by [LH, LV] or [RH, RV] for left (L) or right (R) hand circular transmission respectively, although RCM will offer only right-hand circular transmission. The coherent HH-VV configuration available on TerraSAR-X could also be represented as C2 format.

Polarimetric decomposition methods like Yamaguchi et al. (2011) for fully polarimetric, or m-chi (Raney et al., 2012) for compact polarimetric data, can be applied directly on averaged (speckle filtered) C3 and C2 matrices respectively. These decompositions enhance scattering information, bring it to a more comprehensible level to end users, and raise the performance of thematic classification methodologies. For SAR products that were acquired with single polarization the use of the covariance matrix does not result in superfluous storage requirements, since only the matrix elements that are populated are kept and the diagonal matrix elements are the backscatter intensities. Thus, a single

channel intensity product would yield only one matrix element and the storage needs would not change.

In order to ease the data structure and the metadata in between C3 and C2, Equation 1 should be redefined as Equation 3. Users will have to take care of this non-standard representation when applying their polarimetric analytic tools. “< >” means that ARD matrix elements are speckle filtered. Equation 3 is valid both for dual-linear and quad polarization.

$$C3 \text{ modified } C3m = \begin{bmatrix} \langle |HH|^2 \rangle & \langle HH \cdot HV^* \rangle & \langle HH \cdot VV^* \rangle \\ \langle HV \cdot HH^* \rangle & \langle |HV|^2 \rangle & \langle HV \cdot VV^* \rangle \\ \langle VV \cdot HH^* \rangle & \langle VV \cdot HV^* \rangle & \langle |VV|^2 \rangle \end{bmatrix} \quad \text{Eq. 3}$$

Furthermore, for compact polarimetric data, it is recommended to store them, by simple transformation, under the circular-circular basis, since RR and RL polarizations (Equation 4) permit faster and more intuitive RGB visualizations (R=RR, G=RR/(RR+RL), B= RL).

$$\text{CH-CV} \quad \text{C2 circular } C2c = \begin{bmatrix} \langle |RR|^2 \rangle & \langle RR \cdot RL^* \rangle \\ \langle RL \cdot RR^* \rangle & \langle |RL|^2 \rangle \end{bmatrix} \quad \text{Eq. 4}$$

A2.2: Polarimetric Radar Decomposition (PRD)

Based on the literature, different methodologies allow decomposition of coherent dual-polarization data or fully polarimetric data to meaningful components summarizing the scattering processing with the interacting media. Decomposition techniques are divided in two categories: Coherent and incoherent.

1. **Coherent decompositions** express the scattering matrix by the summation of elementary objects of known signature (ex.: a sphere, a diplane, a cylinder, a helix, ...). They are used mainly to describe point targets which are coherent. As for examples, coherent PRD could be (but not limited to):

- a. Pauli decomposition (3 layers)

$|\alpha|^2$: sphere (odd-bounce interaction) [Intensity]

$|\beta|^2$: 0° diplane (even-bounce interaction) [Intensity]

$|\gamma|^2$: 45° diplane (volumetric interaction) [Intensity]

- b. Krogager decomposition (5 layers) [Krogager, 1993]

$|\kappa_\sigma|^2$: sphere (odd-bounce interaction) [Intensity]

$|\kappa_\delta|^2$: diplane (odd-bounce interaction) [Intensity]

$|\kappa_\eta|^2$: helix [Intensity]

θ : orientation angle [degrees]

ϕ_s : sphere to diplane angle [degrees]

- c. Cameron (nine classes) –non-dimensional layers [Cameron et al., 1996]

Table A2.1.

Classes	ID
Triedral	1
Dihedral	2
Narrow Dihedral	3
Dipole	4
Cylinder	5
¼ wave	6

Right Helix	7
Left Helix	8
Asymmetrical	9

2. **Incoherent decompositions** describe distributed targets in terms of scattering mechanisms and their diversity. They are generated from averaged Covariance, Coherence or Kennaugh matrices. As for examples, incoherent PRD could be (but not limited to):

- a. Based and saved on intensity of scattering mechanisms can be [Freeman and Durden, 1998; Yamaguchi et al., 2011; Raney et al., 2012]

Table A2.2.

Level 2b - Layers [Intensity]	Incoherent Decompositions		
	Freeman-Durden	Yamaguchi	m-chi
Odd-bounce (surface/triedral)	X	X	X
Even-bounce (dihedral)	X	X	X
Random (volumetric)	X	X	X
Helix		X	

- b. Or based on eigenvector-eigenvalue decomposition expressing the diversity of scattering mechanisms [Cloude and Pottier, 1996] and types

H : Entropy [] is the polarization diversity

A : Anisotropy [] is weighted difference between the 2nd and 3^d eigenvalues

α : Odd-even bounce angle [Degrees]

β : orientation angle [Degrees]

A2.3: Polarimetric Radar Decomposition Product Examples

From fully polarimetric covariance matrix ARD format [POL] (Level-2a), it is possible to apply any version of the popular Yamaguchi methodology, which decomposes the polarimetric information under relative intensities of 4 scattering types: Odd bounce, Even bounce, Random (volume) and helix. Figure A2.3.1b) shows HH intensity of a RADARSAT fully polarimetric acquired over a Spanish area. Decomposition using Yamaguchi methodology [Yamaguchi et al., 2011] can be expressed in RGB color composite (Figure A2.3.1c) where Red channel refers to even bounce scattering like urban area; Green channel is random scattering like vegetation; and Blue channel is odd bounce scattering like bare soil. Figure A2.3.1d) is equivalent to c) where radiometric normalisation (terrain flattening) has been applied with the help of the DEM of the scene (Figure A2.3.1a).

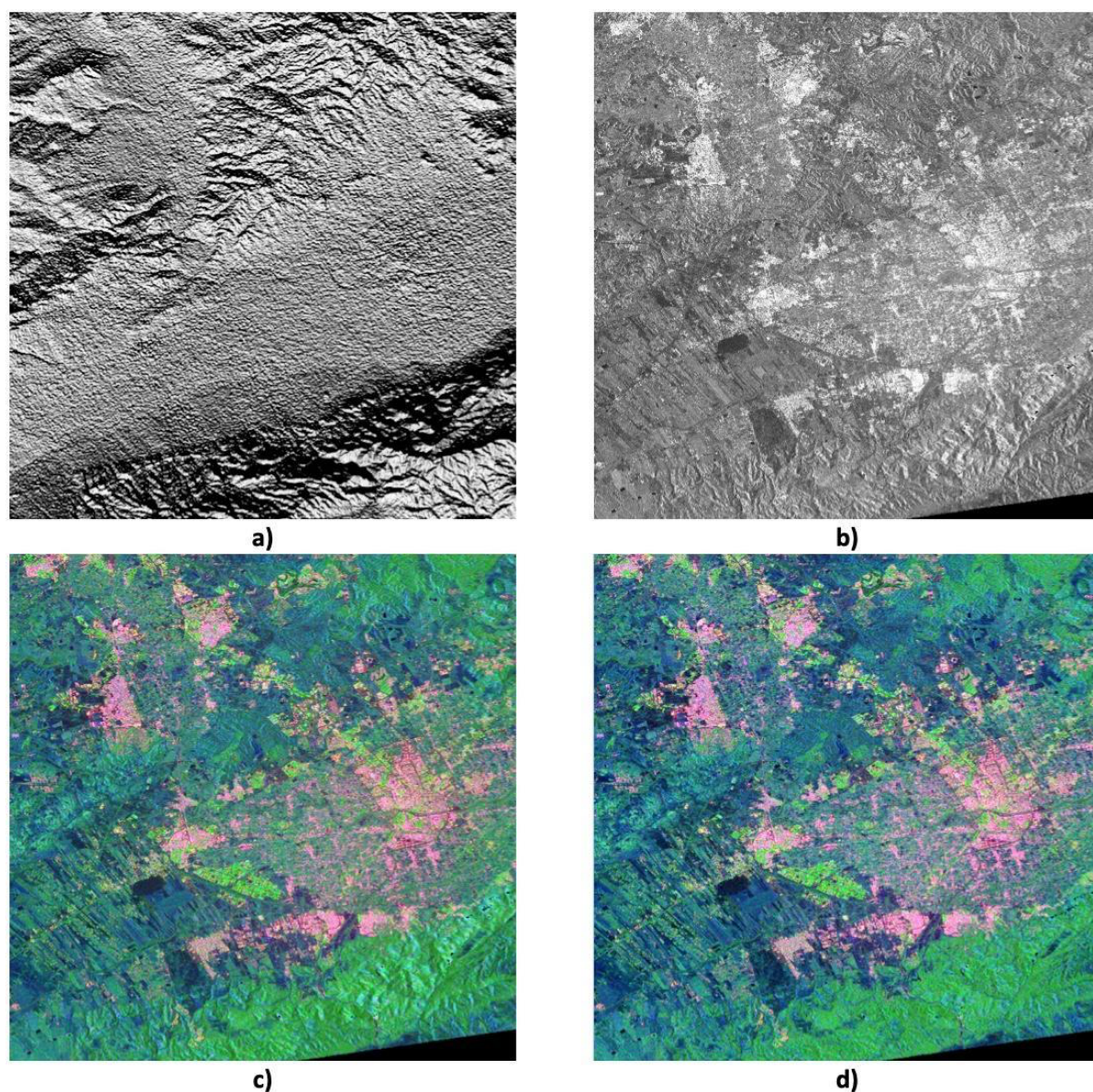


Figure A2.3.1 Example of polarimetric decomposition generated from ARD covariance format. **a)** Shaded DEM of the area; **b)** RADARSAT-2 HH intensity; **c)** Yamaguchi decomposition colour composite (Red: even bounce, Green: random, Blue: odd bounce); **d)** Same as c) with terrain flattening option. Generated from Radarsat-2 FQ18W acquired over Murcia, Spain on 18 June 2014 ©MDA 2014

Figure A2.3.2 is a [PRD] compact polarimetric m-chi decomposition [Raney et al., 2012] simulated from two Canadian prairies Radarsat-2 fully polarimetric scenes acquired in May and June 2012. In May, before the growing season (Figure A2.3.2a), m-chi shows mainly surface scattering from bare soil (blue channel) and vegetation interaction from forested areas (green channel), while in June (Figure A2.3.2b) growth of vegetation modifies the radar signal with interacting media function of the vegetation density and geometry which increase the amount of even bounce (red channel) and random scattering.

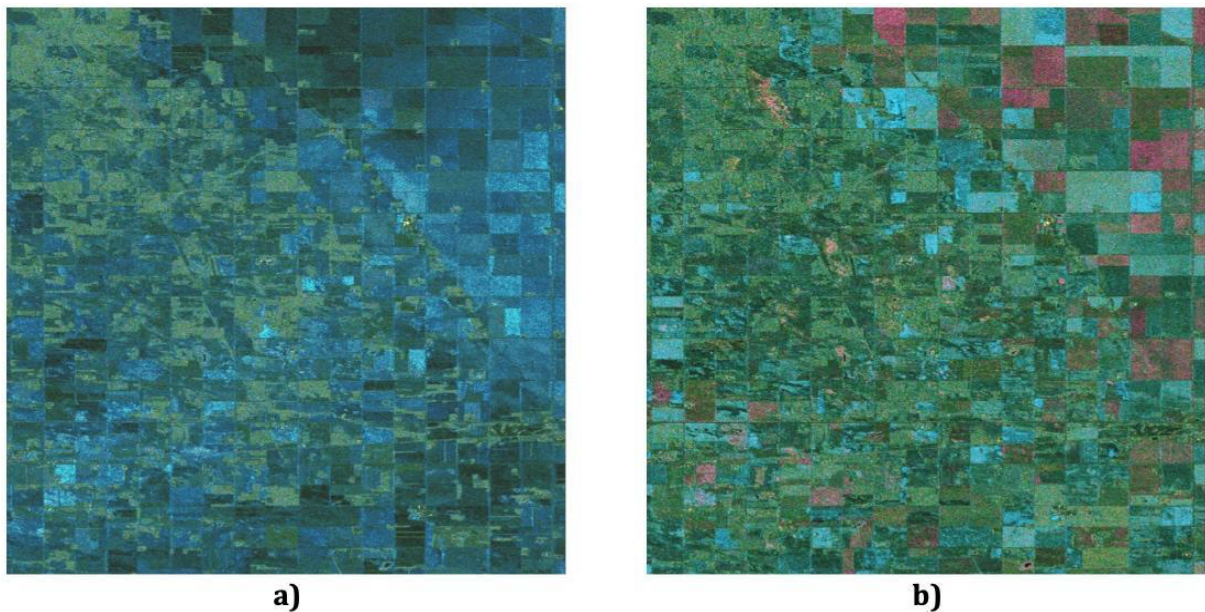


Figure A2.3.2. *m-chi decomposition colour composite of simulated compact polarimetry from Radarsat-2 over an agriculture area. RGB representation: Red: even bounce, Green: random, Blue: odd bounce. a) 3 May 2012; and b) 18 June 2012. Generated from Radarsat-2 FQ6W acquired over SMAPVEX12 campaign Manitoba, Canada on 3 May and 20 June 2012 ©MDA 2012*

Annex 3: Ocean Radar Backscatter [ORB] example

In contrast to [NRB] and [POL], CEOS ARD Ocean Radar Backscatter [ORB] products are geoid corrected and are provided in the Sigma-Nought (σ_E^0) backscatter convention (figure A3.1a), which is recommended for most ocean applications. In addition, availability of the “Local (or Ellipsoidal) Incidence Angle Image” (figure A3.1d)) and “Look Direction Image” per-pixel metadata are highly recommended (otherwise the general metadata “1.7.12 Look Direction Polynomials”) since they required for operational applications like ocean wind field estimates.

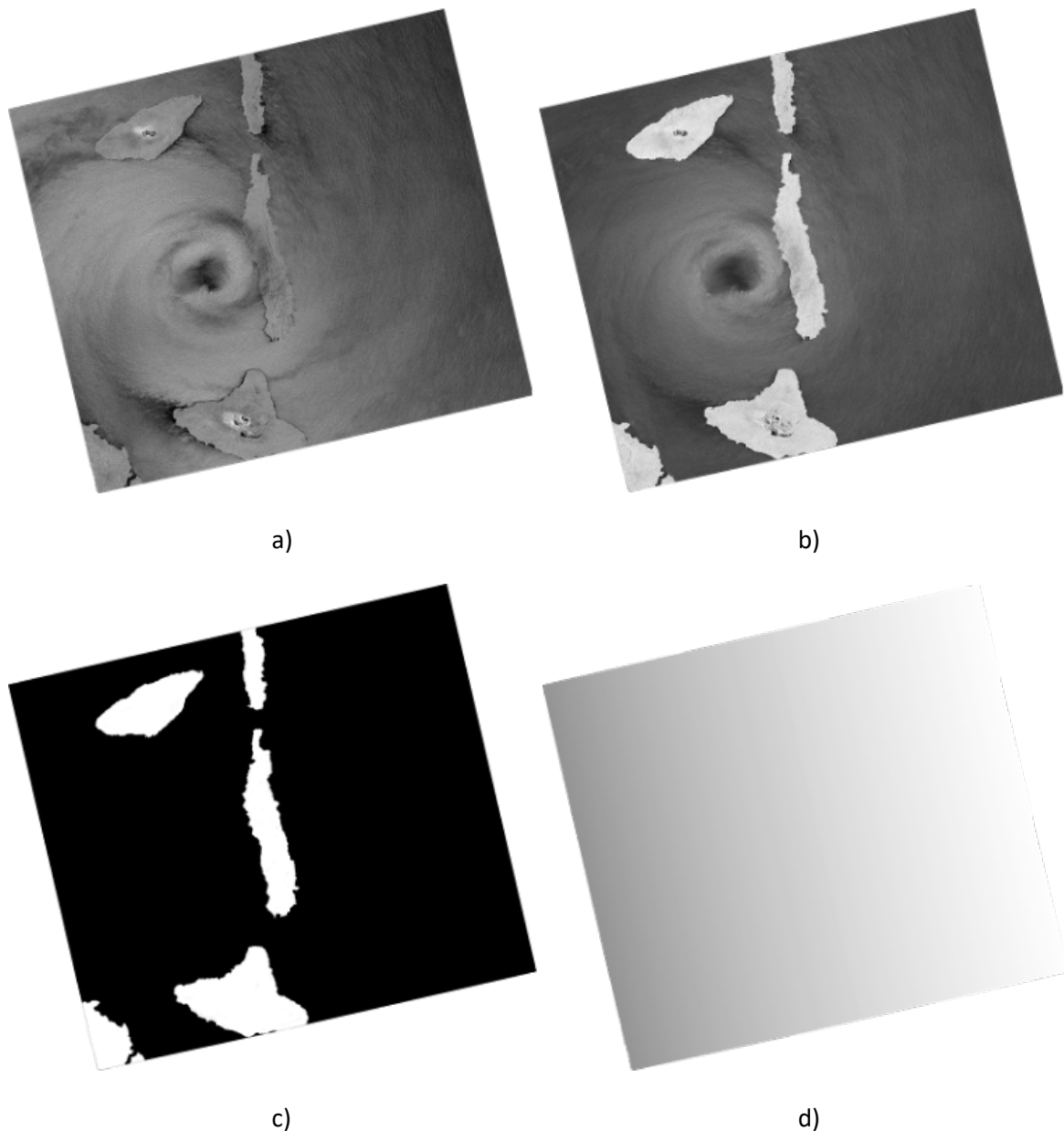


Figure A3.1 Sentinel-1 [ORB] product. Tropical Cyclone Harold passing Vanuatu on April 6, 2020. a) VV intensity b) VH intensity c) Data mask image d) Local incident angle. Processing: A. Rosenqvist (soloEO).

Another useful file is the “Mean Wind-Normalised Backscatter Measurements” (figure A3.2b) which efficiently attenuates intensity variation along range and visually enhances oceanic features. This file is calculated as the ratio between the backscatter intensity and a simulated backscatter intensity image generated using an ocean surface wind model, like CMOD_IRF2 (Quilfen et al, 1998) for VV polarization or CMOD_IRF2K (Vachon and Dobson, 2000) for HH polarization, and the SAR local incidence angle and the look direction information.

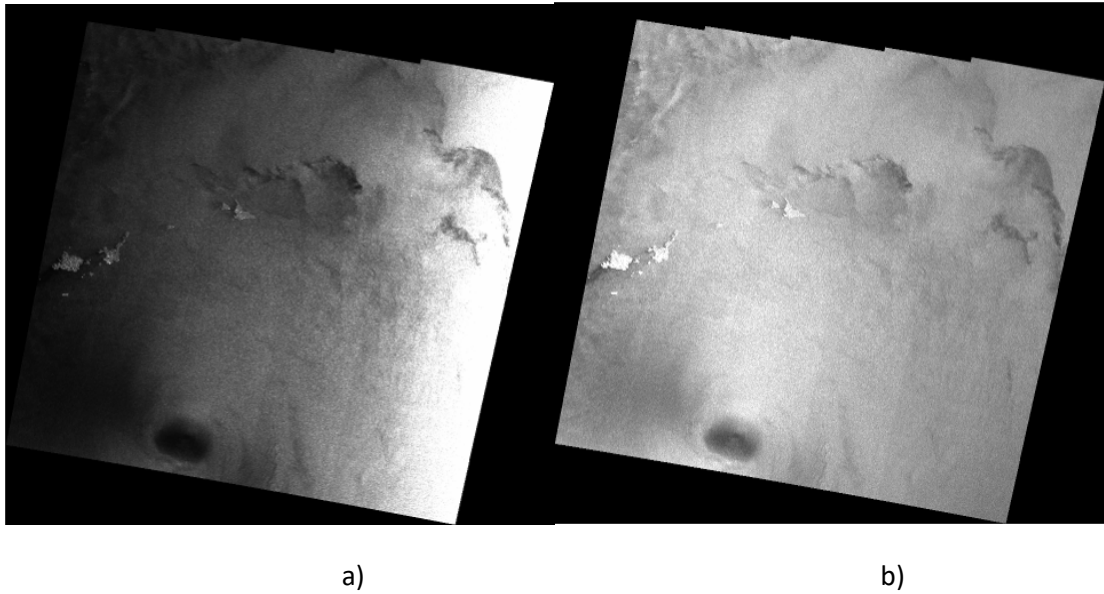


Figure A3.2 Sentinel-1 EW [ORB] product. a) ORB intensity (Sigma-Nought) b) Intensity compensated with the “Mean Wind-Normalised Backscatter Measurement” (i.e not Sigma-Nought) and geocoded. Processing: G. Hajduch (CLS)

Annex 4: Geocoded Single-Look Complex [GSLC] example

In contrast to basic [NRB] and [POL] products, CEOS ARD Geocoded SLC [GSLC] products are kept close to the native resolution in complex data format for which local topographic InSAR phases, relative to a reference orbit (Zebker et al. 2010. Zebker. 2017), have been removed. Having a volume of [GSLC] products acquired over repeat cycles, already radiometric and phase terrain corrected and geocoded (figure A4.1a) and b)), allows user-friendly production of a first iteration of the InSAR coherence (Eq.5 and figure A4.1c) and differential phases (Eq.6 and figure A4.1d) in between [GSLC] pairs, simply by applying local averaging window over the product of a [GSLC] product (GSLC1) with the complex conjugate of a second [GSLC] (GSLC2) divided by their local averaged intensities. These intermediate files could be used for coherent change detection analysis and surface displacement monitoring.

$$\text{Complex coherence: } \rho = \frac{\sum[GSLC_1 * conj(GSLC_2)]}{\sqrt{\sum|GSLC_1|^2 * \sum|GSLC_2|^2}} \quad \text{Eq. 5}$$

The InSAR differential phase (Eq. 6) is the argument of the complex coherence estimated with Eq.5

$$\text{InSAR differential phase: } \varphi = \arg(\rho) \quad \text{Eq. 6}$$

Some advanced [NRB] or [POL] products could include per-pixel “Flattened Phase” data (item 3.7). This “Flattened Phase” enables the possibility to perform InSAR analysis as with two [GSLC] products. As for example, from two different [NRB] products (NRB1) and (NRB2), acquired over repeat cycles (i.e. on the same relative orbit), containing γ_T^0 and their corresponding “Flattened Phase” (FPh1) and (FPh2) per-pixel data, the complex InSAR coherence (Eq.7) can be estimated in the similar manner as Eq. 5 for [GSLC] products.

$$\text{Complex coherence: } \rho_{NRB} = \frac{\sum[(\sqrt{NRB_1} \cdot e^{i \cdot FPh1}) \cdot conj(\sqrt{NRB_2} \cdot e^{i \cdot FPh2})]}{\sqrt{\sum NRB_1 * \sum NRB_2}} \quad \text{Eq. 7}$$

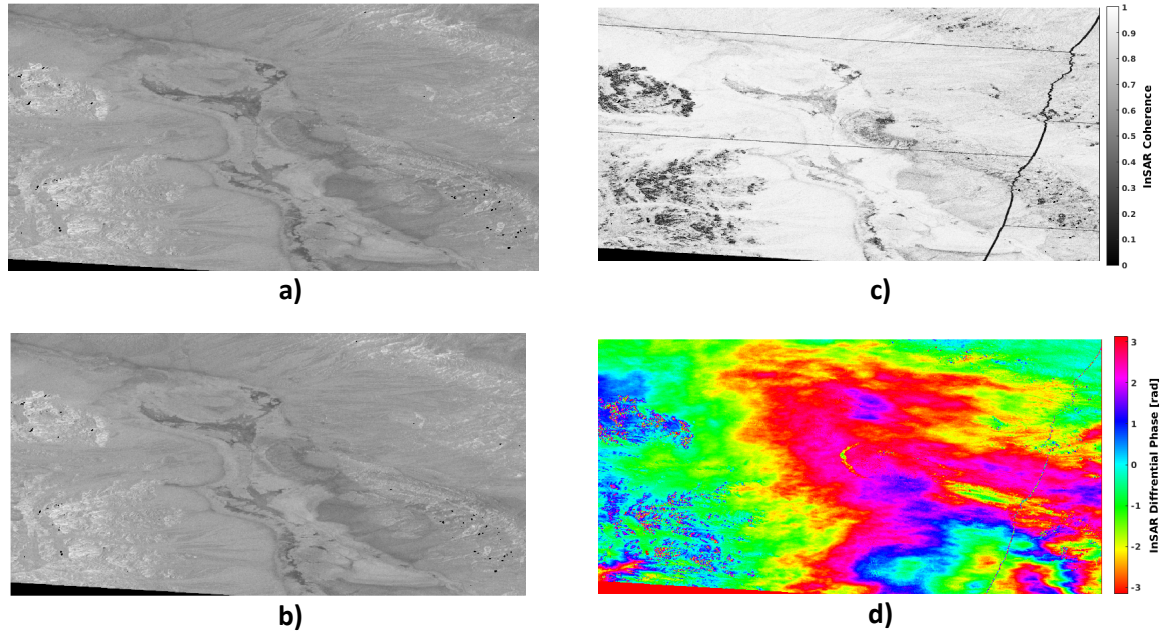
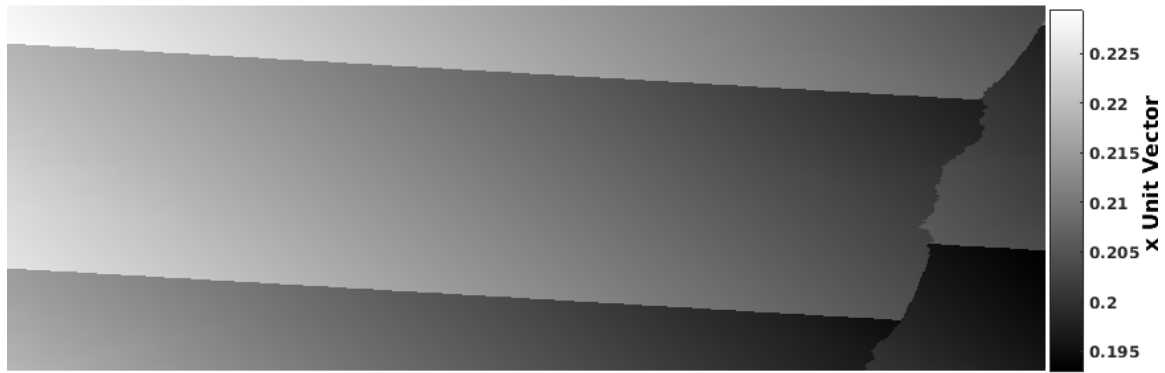
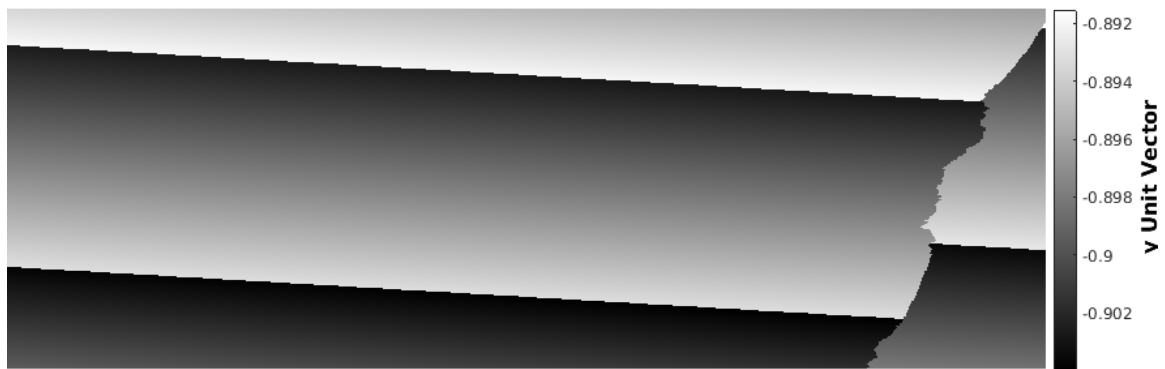


Figure A4.1 Sentinel-1 [GSLC] products example acquired over Death Valley National Park, California, US. **a)** GSLC1: Intensity data of the first [GSLC] product (2017-05-27); **b)** GSLC2: Intensity data of the second [GSLC] product (2017-06-08); **c)** InSAR coherence map generated directly from A4.1a) and b); **d)** InSAR differential phase map generated directly from A4.1a) and b).

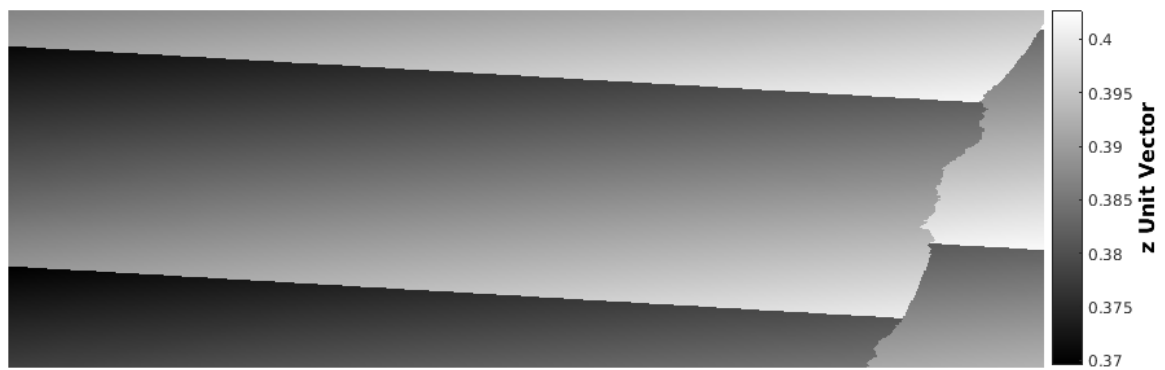
Some advanced [GSLC] product can be provided with “2.12 Radar Unit Look Vector Grid Image” per-pixel metadata (figure A4.2) which gives the accurate 3-D components radar unit look vector used as for example in decomposing the vertical and horizontal component of an InSAR surface displacement estimate.



a)



b)



c)

Figure A4.2 3-D components radar unit look vector of the [GSLC] product in figure A4.1. **a)** x unit component; **b)** y unit component; **c)** z unit component.